Luminescent Properties of Lanthanide Nitrato Complexes with Substituted Bis(benzimidazolyl)pyridines

Stéphane Petoud,[†] Jean-Claude G. Bünzli,*[,†] Kurt J. Schenk,[‡] and Claude Piguet*[,§]

Institute of Inorganic and Analytical Chemistry, BCH, and Institute of Crystallography, BSP, University of Lausanne, CH-1015 Lausanne, Switzerland, and Department of Inorganic, Analytical and Applied Chemistry, Sciences II, University of Geneva, CH-1211 Geneva-4, Switzerland

Received October 31, 1996[⊗]

The protonated form of the ligand 2,6-bis(1′-methylbenzimidazol-2′-yl)pyridine crystallizes as its perchlorate salt (HL^1)ClO_4 (**1**) in the orthorhombic system *Pbca*, with $a = 13.976(3)$ Å, $b = 14.423(3)$ Å, $c = 19.529(4)$ Å, $Z = 8$. The proton is located on one benzimidazole N-atom, and the two N-methyl substituents lie on the same side of the pyridine N-atom (cisoid conformation). New 1:1 nitrato complexes of composition $[Eu(NO_3)_3(L^i)](solv')_y$ have been isolated with L^4 (**4**), L^6 (**5**), L^7 (**6**), and L^8 (**7**), and their structural and photophysical properties are compared with those of the previously reported complexes $[Eu(NO_3)_3(L^1)(MeOH)]$ (**2**) and $[Eu(NO_3)_3(L^3)]$ (**3**). The crystal and molecular structure of $[Eu(NO_3)_3(L^7)(MeCN)]\cdot 2.5MeCN$ at 180 K (**6a**, triclinic, $P\bar{1}$, $a = 12.137(2)$ Å, $b = 14.988(3)$ Å, $c = 16.926(3)$ Å, $\alpha = 114.52(3)°$, $\beta = 98.28(3)°$, $\gamma = 103.99(3)°$, $Z = 2$) shows a decacoordinated Eu^{III} ion to six O-atoms from the nitrates, three N-atoms from L^7, and one N-atom from a coordinated MeCN. The metal-centered luminescence arising upon ligand excitation in the solid state is analyzed in terms of nephelauxetic effects of the ligand and crystal field splitting of the $^7F_1$ level. Quantum yields of 10^{-3} and 10^{-4} M solutions in MeCN are substituent dependent and may be rationalized by taking into account several factors, including the energy of the ligand singlet and triplet levels and the arrangement of the ligands in the first coordination sphere. We also show that the quantum yield of the ligand-centered luminescence decreases in the order $L^1 > [La(NO_3)_3(L^1)]MeOH > [La(L^1)_3](ClO_4)_3$.

Introduction

Several fast developing research themes in the coordination chemistry of lanthanides pertain to the use of their trivalent ions Ln^{III} in biology and medicine.[1,2] The design of time-resolved fluoroimmunoassays,[3] the labeling and the specific cleavage of DNA and RNA,[4,5] the synthesis of efficient shift reagents for NMR spectroscopy and contrast agents for nuclear magnetic imaging,[6] and the development of photosensitizers for cancer therapy[7] are vivid examples of this trend. These applications require precise knowledge of the coordination properties of the lanthanide ions and carefully tailored ligands able to encapsulate these ions while preserving or enhancing some of their spectroscopic and magnetic properties.

We have recently launched a research program aimed at synthesizing building blocks for the design of light-converting devices and materials with predetermined luminescent and/or magnetic properties. The geometric arrangement around Ln^{III} ions essentially depends upon the steric properties of the ligands, coordination numbers between 3 and 12 being easily obtained with a suitable design of ligating molecules and atoms.[8] Despite the diversity reflected by the lanthanide coordination compounds, which entitles Ln^{III} ions to be called the "chameleons of coordination chemistry", these ions have a marked preference for coordination numbers between 8 and 10. In previous parts of this work, we have shown that bis(benzimidazolyl)pyridines L^i (Scheme 1) are well-suited ligands for fulfilling the geometrical requirements of the lanthanide ions. They react with lanthanide nitrates to give neutral and luminescent complexes $[Ln(NO_3)_3(L^i)(solv)]$ ($i = 1-3$)[9] and with perchlorates to yield triple helical $[Ln(L^i)_3]^{3+}$ complexes with a coordination geometry close to the ideal tricapped trigonal prism ($i = 1-5$).[10,11] In the latter complexes, the substituents R^2 have a large influence on the quantum yield of the Eu^{III}-centered luminescence.[11] Moreover the unsymmetric ligands L^9 and L^{10} selectively self-assemble with mixtures of Ln^{III} and M^{II} (M = Zn, Fe) ions, leading to triple-stranded non-covalent heterodinuclear podates $[LnM(L^i)_3]^{5+}$,[12−16] while the binucleating symmetrical ligand L^{11} is coded for the coordination of two 4f ions and gives

[†] Institut de Chimie Minérale et Analytique, Université de Lausanne.
[‡] Institut de Cristallographie, Université de Lausanne.
[§] Université de Genève.
[⊗] Abstract published in *Advance ACS Abstracts,* March 1, 1997.

(1) Bünzli, J.-C. G. In *Lanthanide Probes in Life, Chemical and Earth Sciences. Theory and Practice*; Bünzli, J.-C. G., Choppin, G. R., Eds.; Elsevier Science Publishers B. V.: Amsterdam, 1989; pp 219−93.
(2) Evans, C. H. *Biochemistry of the Lanthanides*; Plenum Press: New York, 1990.
(3) Mathis, G. *Clin. Chem.* **1995**, *41*, 1391.
(4) Komiyama, M. *J. Biochem.* **1995**, *118*, 665.
(5) Häner, R.; Hall, J.; Husken, D.; Moser, H. E. *NATO ASI Ser. C* **1996**, *479*, 307.
(6) Peters, J. A.; Huskens, J.; Raber, D. J. *Prog. Nucl. Magn. Reson. Spectrosc.* **1996**, *28*, 283.
(7) Sessler, J. L.; Kral, V.; Hoehner, M. C.; Chin, K. O. A.; Davila, R. M. *Pure Appl. Chem.* **1996**, *68*, 1291.
(8) Bünzli, J.-C. G. In *Basic and Applied Aspects of Rare Earths*; Caro, P., Saez Puche, R., Eds., in press.
(9) Piguet, C.; Williams, A. F.; Bernardinelli, G.; Moret, E.; Bünzli, J.-C. G. *Helv. Chim. Acta* **1992**, *75*, 1697.
(10) Piguet, C.; Williams, A. F.; Bernardinelli, G.; Bünzli, J.-C. G. *Inorg. Chem.* **1993**, *32*, 4139.
(11) Piguet, C.; Bünzli, J.-C. G.; Bernardinelli, G.; Bochet, C. G.; Froidevaux, P. *J. Chem. Soc., Dalton Trans.* **1995**, 83.
(12) Piguet, C.; Bünzli, J.-C. G.; Bernardinelli, G.; Hopfgartner, G.; Petoud, S.; Schaad, O. *J. Am. Chem. Soc.* **1996**, *118*, 6681.
(13) Piguet, C.; Hopfgartner, G.; Williams, A. F.; Bünzli, J.-C. G. *J. Chem. Soc., Chem. Commun.* **1995**, 491.
(14) Piguet, C.; Rivara-Minten, E.; Hopfgartner, G.; Bünzli, J.-C. G. *Helv. Chim. Acta* **1995**, *78*, 1541.
(15) Piguet, C.; Bernardinelli, G.; Bünzli, J.-C. G.; Petoud, S.; Hopfgartner, G. *J. Chem. Soc., Chem. Commun.* **1995**, 2575.
(16) Piguet, C.; Rivara-Minten, E.; Hopfgartner, G.; Bünzli, J.-C. G. *Helv. Chim. Acta* **1995**, *78*, 1651.

S0020-1669(96)01305-5 CCC: $14.00

Scheme 1

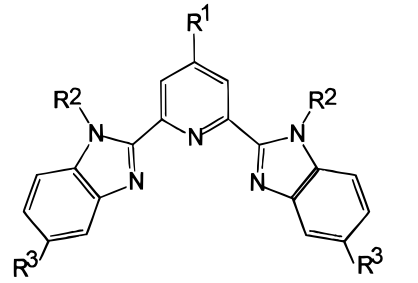

L	R^1	R^2	R^3
L^0	H	H	H
L^1	H	Me	H
L^2	H	Et	H
L^3	H	Oct	H
L^4	H	$Bz(OMe)_2$	H
L^5	H	Et	Me
L^6	Phe	$Bz(OMe)_2$	H
L^7	$PheNO_2$	$Bz(OMe)_2$	H
L^8	$PheNEt_2$	$Bz(OMe)_2$	H

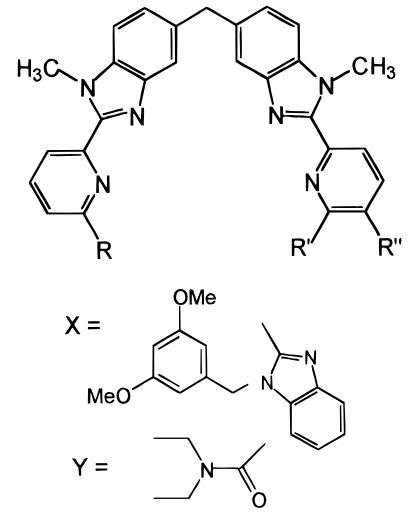

L^9	R = X, R' = H, R'' = Me
L^{10}	R = Y, R' = H, R'' = Me
L^{11}	R = R' = X, R'' = H

pseudo-D_3 triple helical cations $[Ln_2(L^{11})_3]^{6+}$ in which the two 4f ions are located at approximately 8.9 Å.[17,18]

One of our research goals is to unravel the effect of substituents R^1 and R^2 in ligands L^i, $i = 1-8$, on both the structure and the photophysical properties of the Eu^{III} complexes. Since the quantum yield may be substantially affected by stacking interactions between ligand strands in $[Ln(L^i)_3]^{3+}$ complexes,[11] we have investigated the luminescence properties of the 1:1 nitrato complexes $[Ln(NO_3)_3(L^i)(solv)_x]$ ($i = 1$, 3, 4, 6−8). The crystal and molecular structures of $(HL^1)ClO_4$ and $[Eu(NO_3)_3(L^7)(MeCN)]\cdot 2.5MeCN$ are also presented and discussed with respect to the published structures of $[Eu(NO_3)_3(L^1)(MeOH)]$ and $[Eu(NO_3)_3(L^3)]$.[9]

Experimental Section

Solvents and starting materials were purchased from Fluka AG (Buchs, Switzerland) and used without further purification unless otherwise stated. Acetonitrile was treated by CaH_2 and P_2O_5.[19] Dichloromethane (CH_2Cl_2), *N*,*N*-dimethylformamide (DMF), and triethylamine were distilled from CaH_2. Lanthanide nitrates, perchlorates, and trifluoromethanesulfonates (triflates) were prepared from the oxides (Glucydur, 99.99%).[20a] The Ln content of the solid salts was determined by titrations with Titriplex III (Merck) in the presence of urotropine and xylene orange.[20b]

Preparation and Properties of the Ligands. Ligands L^1-L^8 were synthesized according to procedures previously described.[11,21] Systematic nomenclature: 2,6-bis(benzimidazol-2-yl)pyridine, L^0; 2,6-bis-(1′-X-benzimidazol-2′-yl)pyridine, X = methyl, L^1, X = ethyl, L^2, X = octyl, L^3, and X = 3,5-dimethoxybenzyl, L^4 ; 2,6-bis(1′-ethyl-5′-methylbenzimidazol-2′-yl)pyridine, L^5; 2,6-bis[1′-(3,5-dimethoxybenzyl)benzimidazol-2′-yl]-4-[X]-pyridine, X = phenyl, L^6; 4″-nitrophenyl, L^7 ; 4″-(diethylamino)phenyl, L^8. The pK_a's ($\pm 2\sigma$) of L^1 have been determined at 298 K by potentiometric titrations of 2.5×10^{-3} M solutions in 95:5 MeOH:H_2O (v/v) by 0.05 M and 1 M $HClO_4$ in the presence of 0.1 M NEt_4ClO_4 (TEAP): $pK_{a1} = 4.1 \pm 0.1$; $pK_{a2} = 2.9 \pm 0.1$; $pK_{a3} < 2$. Single crystals of $(HL^1)ClO_4$ (**1**) suitable for X-ray diffraction were obtained while attempts were made to crystallize $[Lu(L^1)_3](ClO_4)_3$ out of a solution obtained by mixing 0.07 mmol of $Lu(ClO_4)_3\cdot 7H_2O$ in MeCN and 0.21 mmol of L^1 in 4:1 CH_2Cl_2:MeCN (v/v). A yellow coloration appeared immediately, and a pale yellow solid crystallized after 30 min, which was dried for 5 h (10^{-2} Torr, 40 °C) and dissolved in MeCN at 35 °C. To isolate X-ray quality crystals, Et_2O was diffused during 1−2 days into a concentrated acetonitrile solution.

Preparation of 1:1 Nitrato Complexes. $[Eu(NO_3)_3(L^1)(MeOH)]$ (**2**) and $[Eu(NO_3)_3(L^3)]$ (**3**) have been previously described.[9] $[Eu(NO_3)_3(L^4)]\cdot 2H_2O$ (**4**): A 143 mg (0.33 mmol) amount of $Eu(NO_3)_3\cdot 5.5H_2O$ in 5 mL of MeCN was added to 200 mg (0.33 mmol) of L^4 in 5 mL of CH_2Cl_2. A white precipitate formed immediately. CH_2Cl_2 was evaporated, and the residual suspension was refluxed for 30 min. After cooling and filtration, the white solid was recrystallized in MeCN (280 mg, yield 86%).

The complexes with L^6, L^7, and L^8 were obtained according to the following general procedure. A 0.06 mmol amount of $Eu(NO_3)_3\cdot 3.7H_2O$ in a minimum amount of MeCN was added under vigorous stirring to a solution of 0.06 mmol of L^i in a minimum amount of 4:1−1:1 CH_2Cl_2:MeCN (v/v), depending on the ligand solubility. A coloration change occurred immediately (yellow for L^6 and L^7, orange for L^8). The solution was stirred for 2 h at room temperature, and the solvent was evaporated. The solid was dried for 3 h (10^{-2} Torr, 40 °C) and dissolved in a minimum amount of MeCN at 50 °C under ultrasonic irradiation. The solution was filtered. Crystals were collected either directly (L^7) or after diffusion of ethyl acetate (L^8) or *tert*-butyl methyl ether (L^6) and were dried for 15 h to remove the solvent (10^{-2} Torr, 30 °C). Yields ranged between 50 and 65%. Anal. Calcd for $[Eu(NO_3)_3(L^4)]\cdot 2H_2O$ (**4**), $C_{37}H_{33}N_8O_{13}Eu$ (fw 985.70): C, 45.09; H, 3.78; N, 11.37; Eu, 15.42. Found: C, 45.0; H, 3.8; N, 11.4; Eu, 15.2. Calcd for $[Eu(NO_3)_3(L^6)]\cdot(H_3C)_3COCH_3$ (**5**), $C_{48}H_{49}N_8O_{14}Eu$ (fw 1113.92): C, 51.76; H, 4.43; N, 10.06. Found: C, 51.50; H, 4.50; N, 10.17. Calcd for $[Eu(NO_3)_3(L^7)]$ (**6**), $C_{43}H_{36}N_9O_{15}Eu$ (fw 1070.78): C, 48.23; H, 3.39; N, 11.77. Found: C, 48.10; H, 3.44; N, 11.62. Calcd for $[Eu(NO_3)_3(L^8)]$ (**7**), $C_{47}H_{46}N_9O_{13}Eu$ (fw 1096.90): C, 51.47; H, 4.23; N, 11.49. Found: C, 50.92; H, 4.18; N, 11.08.

Physicochemical Measurements. Electronic spectra in the UV−visible range were recorded at 20 °C from 10^{-3} M acetonitrile solutions with Perkin-Elmer Lambda 5 and Lambda 7 spectrometers using quartz cells of 0.1 and 0.01 cm path lengths. High-resolution luminescence spectra and lifetime determinations were measured on a previously described instrumental setup.[22,23] Samples were measured either as

(17) Bernardinelli, G.; Piguet, C.; Williams, A. F. *Angew. Chem., Int. Ed. Engl.* **1992**, *31*, 1622.
(18) Piguet, C.; Bünzli, J.-C. G.; Bernardinelli, G.; Hopfgartner, G.; Williams, A. F. *J. Am. Chem. Soc.* **1993**, *115*, 8197.
(19) Perrin, D. D.; Armarego, W. L. F. *Purification of Laboratory Chemicals*; Pergamon Press: Oxford, U.K., 1988.
(20) (a) Bünzli, J.-C. G.; Moret, E.; Yersin, J.-R. *Helv. Chim. Acta* **1978**, *61*, 762. (b) Schwarzenbach, G. *Die komplexometrische Titration, Die Chemische Analyse*; F. Enke: Stuttgart, Germany 1957; Vol. 45.
(21) Bochet, C. G.; Piguet, C.; Williams, A. F. *Helv. Chim. Acta* **1993**, *76*, 372.
(22) Guerriero, P.; Vigato, P. A.; Bünzli, J.-C. G.; Moret, E. *J. Chem. Soc., Dalton Trans.* **1990**, 647.
(23) Bünzli, J.-C. G.; Milicic-Tang, A. *Inorg. Chim. Acta* **1996**, *252*, 221.

Table 1. Crystallographic Data for $(HL^1)^+$ (**1**) and $[Eu(NO_3)_3(L^7)(MeCN)]\cdot 2.5MeCN$ (**8**)

	1	**8**		**1**	**8**
formula	$C_{21}H_{18}N_5O_4Cl$	$C_{50}H_{46.5}N_{12.5}O_{15}Eu$	D_{calc} (g cm^{-3})	1.484	1.544
fw	439.85	1214.5	D_{obs} (g cm^{-3}, 20°)	1.48(2)	1.52(2)
cryst syst	orthorhombic	triclinic	$\mu_{Cu\,K\alpha}$ (cm^{-1})	20.77	92.83
space group	*Pbca*	$P\bar{1}$	F(000)	1824	1234
a (Å)	13.976(3)	12.137(2)	θ range (deg)	4.95−59.58	2.99−59.95
b (Å)	14.423(3)	14.988(3)	index range h	$-15 \le h \le 0$	$-13 \le h \le +8$
c (Å)	19.529(4)	16.926(3)	index range k	$-15 \le k \le 0$	$-16 \le k \le +16$
α (deg)	90	114.52(3)	index range l	$-21 \le l \le 21$	$-19 \le l \le +19$
β (deg)	90	98.28(3)	reflns collectd	5207	11359
γ (deg)	90	103.99(3)	indpnt reflcns $I > 2\sigma_i$	2653	7754
V (Å^3)	3936.60(14)	2612.0(8)	ext coeff	0.000 98(5)	0.0011(2)
Z	8	2	goodness of fit on F^2	2.444	1.325
T (°C)	−93	−93	R^a	0.0434	0.0621
λ (Å)	1.54184	1.54184	$R_w{}^b$	0.0854	0.1466

[a] $R = \sum[|F_o| - |F_c|]/\sum|F_o|$. [b] $R_w(F_o^2) = [\sum w(F_o^2 - F_c^2)^2/\sum w(F_o^4)]^{1/2}$.

finely powdered samples (**2**−**4**) or as crystals in ethyl acetate (**7**) or *tert*-butyl methyl ether (**5**, **6**). Luminescence spectra were corrected for the instrumental function but not excitation spectra. Lifetimes are averages of at least three determinations. Quantum yields were determined in anhydrous and degassed acetonitrile with the help of a Perkin-Elmer LS-50 spectrofluorimeter. Relative quantum yields were calculated using the following equation:

$$Q_x/Q_r = [A_r(\lambda_r)/A_x(\lambda_x)][I(\lambda_r)/I(\lambda_x)][n_x^2/n_r^2][D_x/D_r]$$

where subscript r stands for the reference and x for the samples; A is the absorbance at the excitation wavelength, I is the intensity of the excitation light at the same wavelength, n is the refractive index (1.343 for solutions in MeCN and 1.333 for solutions in water), and D is the integrated luminescence intensity. For ligand-centered luminescence, emission band areas were corrected, when needed, for the Rayleigh diffusion band, itself corrected for the absorbance of the solution. The concentrations used were 9.86×10^{-5} M for L^1 ($\lambda_{exc} = 347$ nm), 1.02×10^{-4} M for the 1:1 La^{III} complex ($\lambda_{exc} = 374$ nm), and 1.11×10^{-4} M for the 1:3 La^{III} complex ($\lambda_{exc} = 392$ nm). For metal-centered luminescence, the Eu^{III} emission to the ^7F_J, $J = 0-4$, levels only has been measured, the transition to $^7F_5$ and $^7F_6$ being quite faint; moreover, since measurements were made relative to $[Eu(terpy)_3](ClO_4)_3$ (terpy = 2,2′:6′,2″-terpyridine), the error introduced in neglecting these two transitions is minimized and is evaluated to <5%. The excitation wavelengths have been chosen to meet the conditions pertaining to a linear relationship between the intensity I_f of the emitted light and the concentration c of the absorbing and emitting species: theoretically, ϵbc, where ϵ is the molar absorption coefficient and b the optical path length, should be less than 0.05 to allow higher order terms to be neglected in the I_f versus c relationship.[24] To avoid complex dissociation, we have chosen $10^{-3}-10^{-4}$ M concentrations. The water content of the solutions was checked before and after the measurements by Karl Fischer titrations and never exceeded 50 ppm.

IR spectra were obtained from KBr pellets with a Perkin-Elmer 883 or a Mattson Alpha Centauri FT spectrometer. Elemental analyses were performed by Dr. H. Eder of the Microchemical Laboratory of the University of Geneva.

X-ray Experimental Section. The X-ray crystallographic studies were done using an Enraf-Nonius CAD4 diffractometer (Table 1). Data were collected using the $\theta-2\theta$ mode (scan width, $0.8 + 0.14 \tan\theta$; scan speed, 0.72−4.0 deg·min^{-1}) and were corrected for absorption, polarization, and Lorentz effects. The structures were solved by direct methods and difference Fourier techniques and were refined by full-matrix least-squares with the help of the program package SHELXTL.[25] Other calculations were done with XTAL[26] or PACHA.[27]

X-ray Study for $(HL^1)ClO_4$. A pale yellow crystal was incorporated in perfluorinated oil Hostinert 216. Three standard reflections were measured every 2 h and indicated a total intensity decrease of 10%. Data were corrected for this drift. The unit cell was determined by least-squares refinement on 46 reflections ($45° \le 2\theta \le 52°$). All of the non-hydrogen atoms were refined anisotropically. Positional and isotropic displacement parameters were refined for H-atoms as well. No restraint was applied, and 299 parameters were determined from the 2653 observed reflections. The largest differences amounted to 0.539 and −0.379 e Å^{-3} in the final Fourier difference synthesis.

X-ray Study for $[Eu(NO_3)_3(L^7)(MeCN)]\cdot 2.5MeCN$ (6a). X-ray quality crystals were collected from an acetonitrile solution of **6**, after diffusion of *tert*-butyl methyl ether and were not dried. A yellow crystal was incorporated in perfluorinated oil Hostinert 216 to avoid solvent efflorescence. Three standard reflections were measured every 3 h and indicated a total intensity decrease of 11%. Data were corrected for this drift. The unit cell was determined by least-squares refinement on 25 reflections ($40° \le 2\theta \le 54°$). All of the non-hydrogen atoms were refined anisotropically; H atoms were put into calculated positions and refined isotropically. Disordered acetonitrile was held in place by means of 9 distance restraints, and 701 parameters were determined from the 7754 observed reflections. The largest differences amounted to 2.726 and −1.613 e Å^{-3} in the final Fourier difference synthesis and were located in the vicinity of the Eu atom.

Results and Discussion

Structure of the Protonated Ligand $(HL^1)^+$. Despite several studies on the complexation ability of L^1,[9,10,21,28] no crystal structure of the free ligand has been reported to date. The molecular structure of pale yellow $(HL^1)ClO_4$ (Figure 1; Table 2; Tables S1 and S2, Supporting Information) displays the following main features. (i) The proton is localized on N4, with essentially no interaction with the counteranion, contrary to $(H_2$-qpy$)(PF_6)_2$, where qpy stands for 2,2′:6′,2″:6″,2‴:6‴,2⁗-quinquepyridine, strong H···F interactions force the protons to lie symmetrically with respect to two adjacent N atoms.[29] (ii) The two benzimidazole units form fold angles of about 30.5 and 45.3° with the central pyridine ring, the larger angle corresponding to the protonated benzimidazole. These angles are large compared to those found in complexed L^1 (*vide infra*) or in similar ligands: *e.g.* diprotonated $(H_2qpy)^{2+}$ is almost planar, with a maximum angle between two pyridine rings equal to 6.2°.[29] We also note that the benzimidazole moieties are slightly puckered with CNN triangles folded by 3−4° with respect the benzimidazole mean plane. (iii) The two N-methyl substituents on N2 and N5 lie on the same side of the pyridine

(24) Olsen, E. D. *Modern Optical Methods of Analysis*; McGraw-Hill Book Co.: New York, 1975.
(25) *SHELXTL 5.0*; Siemens Analytical X-Ray Instruments Inc.: Madison, WI, 1993.
(26) Hall, S. R.; Stewart, J. M. *XTAL 3.0 User's Manual*; Universities of Western Australia and Maryland: Nedlands, Australia, and College Park, MD, 1989.
(27) Henry, M. *Program PACHA*, Partial Atomic CHarge Analysis; Laboratoire de Chimie Moléculaire de l'Etat Solide, Université Louis Pasteur: F-67000 Strasbourg, France, 1993.
(28) Piguet, C.; Bocquet, B.; Müller, E.; Williams, A. F. *Helv. Chim. Acta* **1989**, *72*, 323.
(29) Constable, E. C.; Elder, S. M.; Walker, J. V.; Wood, P. D.; Tocher, D. A. *J. Chem. Soc., Chem. Commun.* **1992**, 229.

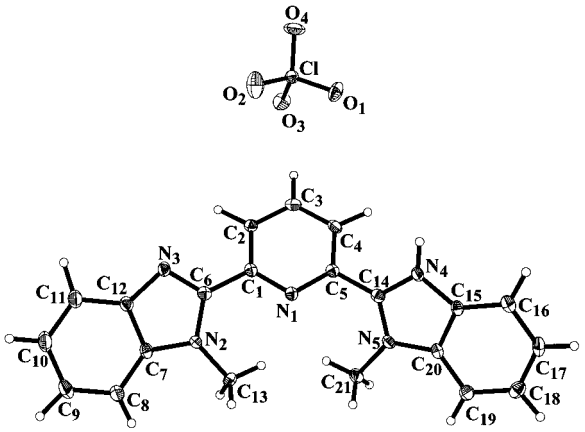

Figure 1. Molecular structure of $(HL^1)^+$ showing the atom-numbering scheme.

Table 2. Selected Bond Lengths (Å) and Angles (deg) in $(HL^1)ClO_4$ (Standard Deviations Indicated within Parentheses)

N1−C1	1.340(4)	N1−C5	1.348(4)
N2−C6	1.362(3)	N2−C7	1.381(4)
N2−C13	1.439(3)	N3−C6	1.308(3)
N3−C12	1.392(4)	N4−C14	1.330(4)
N4−C15	1.399(3)	N5−C14	1.330(3)
N5−C20	1.387(4)	N5−C21	1.454(4)
C1−C2	1.427(3)	C1−C6	1.467(4)
C2−C3	1.388(4)	C3−C4	1.393(4)
C4−C5	1.418(4)	C5−C14	1.475(4)
C7−C12	1.384(3)	C7−C8	1.387(4)
C8−C9	1.369(4)	C9−C10	1.390(4)
C10−C11	1.384(4)	C11−C12	1.382(4)
C15−C20	1.377(4)	C15−C16	1.381(4)
C16−C17	1.376(4)	C17−C18	1.370(4)
C18−C19	1.387(4)	C19−C20	1.382(4)
C1−N1−C5	115.8(2)	C6−N2−C7	109.0(2)
C6−N2−C13	127.3(3)	C7−N2−C13	123.5(2)
C6−N3−C12	106.3(2)	C14−N4−C15	110.3(2)
C14−N5−C20	108.3(2)	C14−N5−C21	125.6(3)
C20−N5−C21	126.0(2)	N1−C1−C2	123.6(3)
N1−C1−C6	117.0(2)	C2−C1−C6	119.4(3)
C3−C2−C1	119.1(3)	C2−C3−C4	118.4(2)
C3−C4−C5	118.0(3)	N1−C5−C4	125.0(3)
N1−C5−C14	116.2(2)	C4−C5−C14	118.8(3)
N3−C6−N2	110.6(3)	N3−C6−C1	123.4(2)
N2−C6−C1	125.9(2)	N2−C7−C12	104.0(2)
N2−C7−C8	133.4(2)	C12−C7−C8	122.5(3)
C9−C8−C7	118.4(3)	C8−C9−C10	119.9(3)
C11−C10−C9	121.3(3)	C12−C11−C10	119.2(3)
C11−C12−C7	118.7(3)	C11−C12−N3	131.3(2)
C7−C12−N3	110.0(2)	N4−C14−N5	108.7(2)
N4−C14−C5	124.6(2)	N5−C14−C5	126.6(3)
C20−C15−C16	122.8(2)	C20−C15−N4	104.4(3)
C16−C15−N4	132.8(2)	C17−C16−C15	116.8(3)
C18−C17−C16	120.8(3)	C17−C18−C19	122.5(3)
C20−C19−C18	116.9(3)	C15−C20−C19	120.2(3)
C15−C20−N5	108.4(2)	C19−C20−N5	131.4(3)

N1-atom, with a contact distance between adjacent H-atoms close to the repulsion limit (H13A−H21A, 1.90 Å). That is, both benzimidazole N3- and N4-atoms are in *trans* position with respect to N1. In ligands derived from terpyridine[30,31] or quaterpyridine,[32] the conformational arrangement around the central pyridine ring has the same *trans, trans* sequence, while

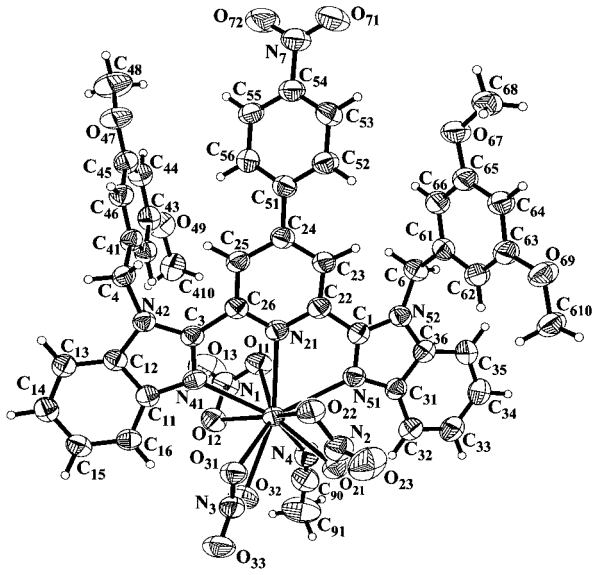

Figure 2. Molecular structure of $[Eu(NO_3)_3(L^7)(MeCN)]\cdot 2.5MeCN$ showing the atom-numbering scheme.

$(H_2qpy)^{2+}$ adopts a *cis, trans, trans, cis* arrangement.[29] In metal complexes, L^1 always displays the *cis, cis* sequence,[33] providing a tridentate binding unit for cation coordination. (iv) Aromatic C−C distances are within the accepted range (mean, 1.382(7) Å), except for two longer bonds in the central pyridine unit, C1−C2 (1.427 Å) and C4−C5 (1.418 Å), involving the 2,6-carbon atoms bearing the benzimidazole substituents. (v) In the crystal, the $(HL^1)^+$ molecules arrange themselves in zigzag layers parallel to the *c* axis (Figure 2) thanks to weak intermolecular interactions between the five-membered ring on the unprotonated benzimidazole unit of one molecule and the six-membered ring of the protonated benzimidazole of the next molecule (C···C or C···N contacts are in the range 3.5−3.7 Å). In this way, each molecule is linked to two others by its benzimidazole arms (Figure F1, Supporting Information). The layers are connected together in the *b*-axis direction by two interactions: an aromatic π-staking interaction between two parallel pyridine rings (fold angle < 1°) situated at a distance of 3.46−3.49 Å and two strong N···H bonds between the unprotonated benzimidazole unit of one molecule and the protonated one of the other molecule, and *vice versa* (N3···N4 = 2.69 Å, N4−H4B−N3 = 171.4°, Figure F2, Supporting Information).

The torsion of the benzimidazole units around the C−C transannular bond and the cisoid arrangement of the N-methyl substituents with respect to the pyridine N1-atom result from a compromise between the maximization of the strong intermolecular interactions depicted in Figure F2 (Supporting Information) and the minimization of the intramolecular methyl−methyl repulsion. The aromatic rings of the $(HL^1)^+$ cation are involved in intermolecular π-interactions. It is a known fact that protonation of this type of ligand induces intermolecular distances and angles compatible with π-stacking interactions, intermolecular distances being much shorter than those (>6 Å) observed in the structure of neutral ligands such as 4′-phenyl-2,2′:6′,2″-terpyridine[31] or 6,6″-dibromo-4′phenyl-2,2′:6′,2″-terpyridine.[34]

Isolation and Structure of 1:1 Nitrato Complexes. As reported earlier for L^1 and L^3,[9] neutral 1:1 complexes form easily

(30) Constable, E. C.; Thompson, A. M. C.; Harveson, P.; Macko, L.; Zehnder, M. *Chem. Eur. J.* **1995**, *1*, 360. Constable, E. C.; Thompson, A. M. C. *New J. Chem* **1992**, *16*, 855.
(31) Constable, E. C.; Lewis, J.; Liptrot, M. C. *Inorg. Chim. Acta* **1990**, *178*, 47.
(32) Constable, E. C.; Elder, S. M.; Healy, D. A.; Tocher, D. A. *J. Chem. Soc., Dalton Trans.* **1990**, 1669.
(33) Piguet, C.; Hopfgartner, G.; Bocquet, B.; Schaad, O.; Williams, A. F. *J. Am. Chem. Soc.* **1994**, *116*, 9092. Piguet, C.; Bocquet, B.; Müller, E.; Williams, A. F. *Helv. Chim. Acta* **1989**, *72*, 323.
(34) Constable, E. C.; Khan, F. K.; Marquez, V. E.; Raithby, P. R. *Acta Crystallogr. Sect. C: Cryst. Struct. Commun.* **1992**, *48*, 932.

Table 3. Selected Bond Lengths (Å) and Angles (deg) in $[Ln(NO_3)_3(L^7)(MeCN)]\cdot 2.5MeCN$ (Standard Deviations Indicated within Parentheses)

Eu−N21	2.629(4)	N1−O11	1.267(6)
Eu−N41	2.526(4)	N1−O12	1.257(6)
Eu−N51	2.554(4)	N1−O13	1.210(7)
Eu−O11	2.478(3)	N2-O21	1.269(6)
Eu−O12	2.540(4)	N2−O22	1.280(6)
Eu−O21	2.449(3)	N2−O23	1.207(7)
Eu−O22	2.487(3)	N3−O31	1.264(5)
Eu−O31	2.520(4)	N3−O32	1.263(6)
Eu−O32	2.555(4)	N3−O33	1.216(6)
Eu−N4	2.555(4)	N4−C90	1.156(8)
N21−Eu−N41	62.4(1)	O11−Eu−O31	144.5(1)
N21−Eu−N51	63.3(1)	O11−Eu−O32	116.4(1)
N21−Eu−O11	66.7(1)	O11−Eu−N4	76.3(1)
N21−Eu−O12	106.4(1)	O12−Eu−O21	137.8(1)
N21−Eu−O21	115.3(1)	O12−Eu−O22	160.6(1)
N21−Eu−O22	70.3(1)	O12−Eu−O31	98.8(1)
N21−Eu−O31	115.7(1)	O12−Eu−O32	68.3(1)
N21−Eu−O32	160.6(1)	O12−Eu−N4	69.1(1)
N21−Eu−N4	131.3(1)	O21−Eu−O22	52.0(1)
N41−Eu−N51	125.7(1)	O21−Eu−O31	69.5(1)
N41−Eu−O11	78.4(1)	O21−Eu−O32	74.2(1)
N41−Eu−O12	70.0(1)	O21−Eu−N4	78.5(1)
N41−Eu−O21	135.9(1)	O22−Eu−O31	67.5(1)
N41−Eu−O22	92.3(1)	O22−Eu−O32	108.2(1)
N41−Eu−O31	73.2(1)	O22−Eu−N4	128.0(1)
N41−Eu−O32	98.7(1)	O31−Eu−O32	49.7(1)
N41−Eu−N4	139.1(1)	O31−Eu−N4	112.9(1)
N51−Eu−O11	78.7(1)	O32−Eu−N4	65.7(2)
N51−Eu−O12	124.7(1)	O11−N1−O12	116.9(4)
N51−Eu−O21	72.3(1)	O11−N1−O13	120.5(5)
N51−Eu−O22	71.8(1)	O12−N1−O13	122.6(5)
N51−Eu−O31	135.8(1)	O21−N2−O22	116.2(4)
N51−Eu−O32	135.5(1)	O21−N2−O23	121.7(5)
N51−Eu−N4	79.6(1)	O22−N2−O23	122.0(5)
O11−Eu−O12	50.8(1)	O31−N3−O32	115.3(4)
O11−Eu−O21	144.3(1)	O31−N3−O33	122.2(4)
O11−Eu−O22	135.4(1)	O32−N3−O33	122.4(4)

upon mixing equivalent amounts of hydrated lanthanide nitrates and ligands L^i in a CH_2Cl_2:MeCN mixture. The general formula of the complexes is $[Ln(NO_3)_3(L^i)(solv)_x]\cdot(solv')_y$ ($x = 0, 1$; $y = 0-2.5$), where the solvent molecule solv sometimes completes the inner shell of the lanthanide ion to a coordination number of 10 but can be removed by heating under vacuum. In order to test the influence of the para substituent R^1 of the central pyridine unit on the light-harvesting properties of the Eu-containing complexes, we have synthesized the new 1:1 nitrato complexes with L^4 and L^6-L^8. The influence of the bulky substituents R^1 and R^2 on the conformation of the bis(benzimidazolyl)pyridine framework has been examined by determining the crystal and molecular structure of $[Eu(NO_3)_3(L^7)(MeCN)]\cdot 2.5MeCN$ (**6a)** at 180 K and comparing it to the structures already published, $[Eu(NO_3)_3(L^1)(MeOH)]$ (**2)** and $[Eu(NO_3)_3(L^3)]$ (**3)**.[9] The atom-numbering scheme for **6a** is given in Figure 2, while selected bond distances and angles are collected in Table 3. Atomic coordinates, anisotropic displacement parameters, and least-squares planes are reported in the Supporting Information (Tables S3−S5). The structure consists of neutral molecules in which Eu^{III} is decacoordinated, being bonded on one side to six O-atoms from the three bidentate nitrate ions and one N-atom from the solvating molecule and on the other side by the three N-atoms from L^7. Uncoordinated and disordered MeCN molecules are also present. The ligating benzimidazole N-atoms adopt a *cis*−*cis* conformation with respect to the nitrogen atom N1, and ligand L^7 is bent, with two different angles between the central pyridine unit and the benzimidazole moieties (4.3 and 13.1°), in contrast to the situation found in complexes **2** (6.5 and 6.2°) and **3** (28.3 and 29.7°). In $[Eu(NO_3)_3(L^1)(MeOH)]$, two intermolecular interactions occur, an aromatic stacking between one benzimidazole unit and the pyridine ring of another molecule, and an H-bond between MeOH and an $O(NO_3)$-atom of another molecule. The methyl substituents do not interfere in this arrangement, allowing a slight but symmetrical bend of the ligand. The long octyl arms of L^3 substantially modify the situation, and crystals of $[Eu(NO_3)_3(L^3)]$ consist of two alternate layers, one containing Eu^{III} and the ligand skeleton, and a second one, lipophilic and filled with the octyl substituents; the π-stacking is considerably weakened, while the bending of the ligand is increased although it remains symmetrical.[9] In $[Eu(NO_3)_3(L^7)(MeCN)]\cdot 2.5MeCN$, the bulky dimethoxybenzyl substituents induce strong intermolecular interactions with nitrate ions (Figure F3, Supporting Information) which could be responsible for the asymmetric conformation of the two benzimidazole units: (i) O21···C610 = 2.90 Å and O21−H61A−C610 = 95.8° and (ii) O13···C68 = 2.97 Å and O13−H68B−C68 = 110°. In addition several weaker interactions occur (Table S6, Supporting Information) as well as an intermolecular π-stacking between the benzimidazole groups (contact distances 3.46−3.76 Å, Figure 5). The planar dimethoxybenzyl substituents are closely packed in the crystal and lie above and below the pseudoplane containing the pyridine ring and the two benzimidazole substituents.

The ligand L^7 is coordinated in the usual meridional planar way and atoms N21, N41, N51, and Eu form a plane in which the bonding O32 atom of one nitrate group also rests (deviation 0.05 Å). As previously observed with L^0, L^1, and L^3, the two Eu−N(benzimidazole) bonds are asymmetric and shorter than the Eu−N(pyridine) distance (Table 4), in contrast to the situation met in 1:3 complexes $[Eu(L^i)_3]^{3+}$ ($i = 1, 5$), where the central pyridine is more tightly bonded. Electronic effects in the ligand are reflected in the mean Eu−N distance, which is longer in **6a** than in **2** and **3**, a consequence of the electron-attracting *p*-nitrophenyl group, but slightly shorter than that in $[Eu(NO_3)_2(L^0)_2]NO_3$.[35] The overall mean Eu−N distance remains, however, shorter in **6a** than in the nine-coordinate $[Eu(terpy)_3]^{3+}$ and $[Eu(terpy)(DPM)_3]$ (DPM = dipivaloylmethanate) complexes (2.60[36] and 2.65 Å,[37] respectively), suggesting that the replacement of the pyridine side arms in terpy by benzimidazole units increases the size of the cavity of the tridentate ligand, permitting a closer approach of the Eu^{III} ion. As a consequence, the bite angles in **6a, 2**, and **3** (average around 63°) are larger than that in $[Eu(terpy)(DPM)_3]$ (61.5°). In **6a**, the acetonitrile molecule is coordinated between the three bidentate nitrates with a bond distance (2.56 Å) close to that reported for $[Sm(MeCN)_9]^{3+}$ (2.54(1) Å).[38] All three nitrate ions have approximate C_{2v} local symmetry and are bonded in an asymmetrical way, especially $(N1)O_3$ and $(N2)O_3$ which are involved in H-bonding (*vide supra*). The Eu^{III} coordination polyhedron is fairly distorted and best described as a 4:5:1 polyhedron similar to the arrangement observed in $[Eu(NO_3)_3(L^1)(MeOH)]$, the O-atom of the methanol molecule being replaced by the N-atom from the acetonitrile molecule. The four-atom plane consists of O12 from $(N1)O_3$, O31 and O32 from $(N3)O_3$, and N41 from one benzimidazole substituent. The three other O-atoms from the nitrates and two N-atoms from the central pyridine and from the coordinated acetonitrile molecule form the five-atom plane, while the coordinating

(35) Wang Shuangxi; Zhu Ying; Cui Yuxin; Wang Liufang; Luo Qinhui. *J. Chem. Soc., Dalton Trans.* **1994**, 2523.
(36) Durham, D. A.; Frost, G. H.; Hart, F. A. *J. Inorg. Nucl. Chem.* **1969**, *31*, 833.
(37) Thompson, L. C.; Holz, R. C. *Inorg. Chem.* **1988**, *27*, 4640.
(38) Hu Jingyu; Shen Qi; Jin Zhongsheng. *Kexue Tongbao (Chin. Sci. Bull.)* **1990**, *35*, 1090.

Table 4. Coordination Number (CN) of Eu^{III}, Selected Eu−X (X = N, O) Bond Lengths (Å), and Effective Ionic Radii (Å) of Eu^{III} in Various Complexes

complex	CN	Eu−N pyridine	Eu−N benzimidazole	Eu−N av	Eu−O(nit) av	R_i[a]	ref
$[Eu(NO_3)_3(L^7)(MeCN)]$	10	2.629	2.536, 2.554	2.57(5)	2.50(4)	1.16	*b*
$[Eu(NO_3)_3(L^1)(MeOH)]$	10	2.611	2.477, 2.537	2.54(6)	2.52(8)	1.17	9
$[Eu(NO_3)_2(L^0)_2]NO_3$	10	2.621[c]	2.555[c]	2.58(4)	2.55(6)	1.17	35
$[Eu(NO_3)_3(L^3)]$	9	2.598	2.491, 2.473	2.52(7)	2.46(2)	1.12	9
$[Eu(L^1)_3](ClO_4)_3$	9	2.576[d]	2.592, 2.613	2.59(2)		1.13	10
$[Eu(L^5)_3](ClO_4)_3$	9	2.563[d]	2.603[c]	2.59(4)		1.13	11

[a] According to Shannon's definition,[39] with $r_N = 1.46$ Å and $r_O = 1.31$. Accepted mean values: 1.12 and 1.18 Å for nona- and decacoordinated Eu^{III}, respectively. [b] This work. [c] Average of the different Eu−N bond lengths. [d] C_3-symmetry, one Eu−N(py) bond length.

Table 5. Ligand Absorptions in Solution (293 K) above 300 nm and Ligand Singlet and Triplet State Energies As Determined from Emission Spectra of the Solids at 77 K

Ligand	solvent[a]	$\pi \rightarrow \pi^*$ E (cm^{-1}) [ϵ $M^{-1}\cdot cm^{-1}$]	$^1\pi\pi^*$ (cm^{-1})	$^3\pi\pi^*$ (cm^{-1})
L^1	MeCN, PC	31 150 (32 000)[b,c]	26 040	21 300
			21 050 (sh)[c]	
L^3	PC	31 150 (30 000)[c]	27 250 (sh)	19 920 (sh)
			26 110	19 085
			24 876 (sh)	
L^4	$CHCl_3$	35 185 (21 450, sh)[d]	23 810	18 655
		30 980 (31 220)	27 725 (sh)	17 485
			20 880 (sh)	
L^6	MeCN	35 290 (34 640)	23 529	18 215
		30 210 (26 650, sh)	22 321 (sh)	
L^7	MeCN	35 210 (38 875, sh)	23 475	18 905
		33 225 (44 790)	23 320	
		28 735 (17 730, sh)	21 140 (sh)	
L^8	$CHCl_3$	35 410 (25 440, sh)	22 025	18 555
		30 770 (33 710)	21 055 (sh)	17 515 (sh)
		26 710 (32 290)[d]	18 975 (sh)	

[a] PC = propylene carbonate (4-methyl-1,3-dioxolan-2-one). [b] From ref 10. [c] From ref 9. [d] From ref 21.

N-atom from the second benzimidazole lies in the capping position. By contrast, the polyhedra for **6a** and **2** are different from the geometrical arrangement observed in the 1:2 complex with L°, which can be described as a distorted bicapped square antiprism.[35] The ionic radius calculated according to Shannon's definition[39] (Table 4) is the same as in the other decacoordinated complexes and is in agreement, within experimental errors, with the value extrapolated for 10-coordination (1.18 Å).[39]

Photophysical Properties of the Ligands. The investigated ligands present a strong $\pi \rightarrow \pi^*$ absorption in the range 31 000−35 000 cm^{-1} which shifts at slightly lower energy and splits into two components upon complexation. They also display two luminescence bands, one between 22 000 and 26 000 cm^{-1} assigned to a $^1\pi\pi^*$ state, while the other, between 18 000 and 21 000 cm^{-1}, corresponds to an emission from a $^3\pi\pi^*$ state. The energy of the triplet state is close to those of the $^5D_0$ (17 240 cm^{-1}) and $^5D_1$ (around 19 000 cm^{-1}) levels of the Eu^{III} ion, a situation favorable for efficient energy transfers between the ligand $^3\pi\pi^*$ state and the excited metal ion states. Relevant data are reported in Table 5, while more detailed discussions of the photophysical properties of L^i have been presented elsewhere.[9−11,21]

Luminescence Properties of the 1:1 Nitrato Complexes in the Solid State. Upon excitation through the $^1\pi\pi^*$ level(s) of the ligands, all of the studied complexes display exclusively the Eu^{III}-centered $^5D_0 \rightarrow {}^7F_J$ ($J = 0-4$) emission bands (Figure F4, Supporting Information), indicating efficient energy transfers from the ligand to the Eu^{III} ion, probably via the $^3\pi\pi^*$ state which is conveniently located 1000−4000 cm^{-1} above the Eu-($^5D_{0,1}$) states. The emission spectra are typical of species with low metal-ion site symmetry, and they are dominated by the hypersensitive $^5D_0 \rightarrow {}^7F_2$ transition (Table 6). The presence of several vibronic transitions and, for the complexes with L^4, L^6, and L^8, of two different metal-ion sites prevents a detailed analysis of the crystal field levels, except for $^7F_1$ for which the main three components could be assigned for each complex. The splitting pattern differs from one ligand to the other, indicating different crystal field strength and symmetry, the larger splitting occurring for L^6 and L^7 and the smaller for L^4. In line with these observations, the $^5D_0 \leftarrow F_0$ transition, measured at 295 K upon monitoring the transitions to either $^7F_1$ or $^7F_2$ (Figure F5, Supporting Information), displays one band for **2**, **3**, and **6a** and two for **4**, **5**, and **7**. Selective excitation on the components of the 0−0 transition yields emission spectra with similar relative intensities for the $^5D_0 \rightarrow {}^7F_J$ transitions, but with somewhat different crystal field patterns. Comparable situations have been reported for $[Eu(L^i)_3]^{3+}$ (i = 1, 2).[10,11] The lines of the 0−0 transition become much narrower at 10 K (fwhh between 0.9 and 3.3 cm^{-1}), but they are often accompanied by satellites which may arise from slightly different Eu^{III} environments created by a change in the intermolecular interactions or by a phase transition induced by the lowering of temperature. Frey and Horrocks recently proposed a correlation between the energy of the 0−0 transition, that is, the position of the $^5D_0$ level, and parameters describing the ability δ of coordinating atoms to produce a nephelauxetic effect: $\tilde{\nu} - \tilde{\nu}_0 = C_{CN}\sum_i n_i\delta_i$, where C_{CN} is a coefficient depending upon the Eu^{III} coordination number (1.0 for CN = 9; 0.95 for CN = 10), n_i the number of atoms of type i, and $\tilde{\nu}_0$ = 17 374 cm^{-1} at 295 K [40] (the temperature dependence of $\tilde{\nu}$ is approximately 1 cm^{-1}/24 K).[1] The parameters δ are tabulated for several functional groups.[40] We have recently demonstrated that an heterocyclic N-atom (HN) tends to produce a larger nephelauxetic effect than an amine N-atom (−12.1)[40] and have deduced from our work on nine-coordinate triple-helical complexes with the benzimidazole-containing ligands L^1, L^2, L^5, and L^9−L^{11} a δ_{HN} parameter equal to −15.3.[12,14] Taking the latter value into account, as well as $\delta_{OH} = -11.6$,[40] $\delta_{O(NO3)} =$

Table 6. Corrected Relative Intensities of the $^5D_0 \rightarrow {}^7F_J$ Transitions and Energies of the Identified $^7F_1$ Sublevels (cm^{-1}) in $[Eu(NO_3)_3(L^i)(solv)_x](solv')_y$, As Measured at 10 K

compd, L^i	$J = 0$ [a]	$J = 1$ [b]	$J = 2$ [b]	$J = 3$ [b]	$J = 4$ [b]	$^7F_1$ levels[b]
2, L^1	0.02	1.0	5.4	0.16	0.44	315, 365, 430
3, L^3	0.01	1.0	7.3	0.30	0.15	321, 359, 421
4, L^4	0.03	1.0	9.1	0.13	0.95	310, 384, 410
5, L^6	*c*	1.0	5.6	0.11	1.29	297, 331, 474
6, L^7	0.03	1.0	5.3	0.24	1.43	258, 396, 454
7, L^8	0.09	1.0	10.5	0.09	1.38	304, 385, 424

[a] Measured on spectra excited through the ligand $^1\pi\pi^*$ state. [b] Measured on spectra excited through the $^5D_0 \leftarrow {}^7F_0$ transition. [c] Too weak to be measured.

(39) Shannon, R. D. *Acta Crystallogr.* **1976**, *A32*, 751.

(40) Frey, S. T.; Horrocks, W. deW., Jr. *Inorg. Chim. Acta* **1995**, *229*, 383.

Table 7. Energy (cm^{-1})[a] of the $^5D_0$(Eu) Level from Emission and Excitation Spectra at 295 K and Calculated from a Theoretical Relationship (See Text)

compd, L^i	excitation	emission	calcd
2, L^1	17 237 (6.5)	17 237 (7.4)	17 244
3, L^3	17 231 (7.6)	17 230 (7.4)	17 248
4, L^4	17 231 (8.3)	17 229 (13)	17 248
	17 248 (10.4)	17 243 (sh)	
5, L^6	17 229 (9.8)	17 226 (10.7)	17 248
	17 248 (11.6)		
6, L^7	17 252 (8.9)	17 243 (8.9)	17 241
7, L^8	17 228 (3.9)[b]	*c*	17 248
	17 238 (3.0)[b]		

[a] Full width at half-height is given between parentheses; sh = shoulder. [b] At 10 K. Adjusted values for 295 K: 17 240 and 17 250 cm^{-1}. [c] Too weak to be measured.

-13.3,[40] and $\delta_{MeCN} = -14.4$,[23] we find the theoretical energies reported in Table 7. The agreement with the experimentally determined energies is satisfying, except that for compound **3**. For the other complexes, one observed transition always falls within less than 10 cm^{-1} of the predicted value. The relationship is unfortunately not precise enough to reflect accurately the electronic changes in the ligands upon changing the substituents R^1 and R^2 and to allow us to determine different δ values for the differently substituted ligands. The discrepancy for compound **3** could be due to the shorter Eu−N distances (Table 4), but it is not the first one we observe. For instance, the energy of the 0−0 transitions for $M_2[Eu(NO_3)_5]$ estimated from the emission spectra at 77 K amounts to 17 228 cm^{-1} for $M = Phe_4As^+$ (17 237 cm^{-1} at 295 K) and 17 252 cm^{-1} for $M = Phe_3EtP^+$ (17 262 cm^{-1} at 295 K), while the two compounds have similar structures with a decacoordinated Eu^{III} ion.[41] The $\delta_{O(NO_3)}$ parameter cited above perfectly reproduces the first value. The discrepancy may arise from the fact that in compounds where the forbidden 0−0 transition is extremely weak the observed band does not necessarily correspond to the electronic transition but could arise from a vibronic contribution from lattice phonons.[42] Other secondary effects may eventually also influence the energy of this transition, *e.g.*, second sphere effects induced by intermolecular interactions or by the electric field from the counterion.

The lifetimes of the $^5D_0$(Eu) excited state measured at 10 K upon direct excitation of this level range between 0.83 and 1.33 ms (Table 8). They decrease only marginally (10−20%) upon increasing the temperature to 295 K. Excitation through the ligand levels yields essentially the same data, indicating a fast energy transfer from the ligand to the 4f states, except for the complex with L^6 where the lifetime is 34% longer. The lifetime for $[Eu(NO_3)_3(L^4)]\cdot 2H_2O$ (1.15 ms) is larger than the one for $[Eu(NO_3)_3(L^1)(MeOH)]$ (0.83 ms), meaning that the solvating water molecules remain in the outer coordination sphere of the metal ion.

Relative Quantum Yields of $[Eu(NO_3)_3(L^i)]$ Solutions in Acetonitrile. We have determined the quantum yields using $[Eu(terpy)_3](ClO_4)_3$ as a secondary standard (Figure 3) rather than $[Ru(bipy)_3](ClO_4)_2$ (bipy = 2,2′-bipyridyl) as is usually reported by other research groups,[43] because the emission and excitation spectra of the former complex better match those of the investigated samples. Moreover, since the weak transitions to $^7F_5$ (around 750 nm) and $^7F_6$ (around 820 nm) are not taken into account, the error due to this neglect is minimized. The quantum yield of 10^{-3} M $[Eu(terpy)_3](ClO_4)_3$ in anhydrous acetonitrile was found to be 1.3% when 10^{-3} M $[Ru(bipy)_3](ClO_4)_2$ in air-saturated water is taken as reference (2.8%).[44] The quantum yields for $[Eu(NO_3)_3(L^i)]$ (i = 1, 3, 4, 6, and 7) determined under ligand excitation are reported in Table 9 and are compared to those obtained for the corresponding 1:3 complexes[11] and for the heterodinuclear EuZn complexes with L^9 and L^{10}.[12] All of the absolute measured quantum yields are low compared for instance to those for solutions of europium trinitrate: 5% for $Eu(NO_3)_3\cdot 6H_2O$ in MeOH[45] and 27.5% for $Eu(NO_3)_3$ in anhydrous acetonitrile.[46] Therefore, although the ligands appear to transfer quantitatively the energy of their excited states onto the europium ion, since no ligand emission from either the $^1\pi\pi^*$ or $^3\pi\pi^*$ states is observed, efficient deexcitation processes take place within the complex molecule. Some of these processes may occur within the bonded ligand molecules themselves, in particular radiationless energy degradation through interactions between the ligand strands. Other radiationless energy degradation mechanisms involve the metal ion, for instance the $^5D_0$(Eu) level is easily quenched by high-energy vibrations,[1,47] or by mixing of the 4f levels with either the ligand-to-metal charge-transfer state,[48] as reported recently in dinuclear complexes with substituted calix[8]arenes,[49,50] or with the ligand states. Regarding the latter process, we have noticed that the relative quantum yields of solutions of europium mixed complexes with phenanthroline and substituted β-diketonates decrease by a factor 64 when the ligand absorption band is shifted from 30 300 to 25 600 cm^{-1}. Similar considerations were put forward by Reinhoudt and co-workers when designing new sensitizer-modified calix[4]arenes enabling near-UV excitation of complexed luminescent lanthanide ions.[51] This phenomenon is confirmed with the presently discussed systems since solutions of $[Eu(NO_3)_3(L^8)]$ give rise to no observable luminescence at room temperature contrary to all of the other complexes, this compound being the only one displaying a low-lying absorption band around 460 nm in addition to the two bands centered around 300 and 350 nm (Figure 3). The absorption spectra of the other solutions display only the latter two transitions occurring at roughly the same energy, except for $[Eu(NO_3)_3(L^7)]$ for which the less energetic transition extends more toward longer wavelengths, and, effectively, this complex possesses the smaller quantum yield of the series. The ligand-to-metal charge-transfer transition could not be located precisely for the investigated complexes, being hidden under the more intense ligand transitions.

In our previous work, we have found that an important factor leading to very low quantum yields for the 1:3 complexes $[Eu(L^i)_3]^{3+}$ is apparently associated with the triple helical structure of these edifices, resulting in strong intermolecular interactions between the ligand strands: addition of water, a strong quencher of the $^5D_0$(Eu) level, to the solutions caused an increase in luminescence intensity as a result of ligand dissociation.[11] The data of Table 9 for the 1:1 nitrato complexes 10^{-3} M in acetonitrile are consistent with this finding since the quantum yields are 3−4 orders of magnitude larger than those of the corresponding triple helical edifices. On the other hand they

(41) Bünzli, J.-C. G.; Klein, B.; Pradervand, G.-O.; Porcher, P. *Inorg. Chem.* **1983**, *22*, 3763.
(42) Harrison, M. T.; Denning, R. G.; Davey, S. T. *J. Non-Cryst. Solids* **1995**, *184*, 286.
(43) Casnati, A.; Fischer, C.; Guardigli, M.; Isernia, A.; Manet, I.; Sabbatini, N.; Ungaro, R. *J. Chem. Soc., Perkin Trans. 2* **1996**, 395.
(44) Nakamaru, K. *Bull. Chem. Soc. Jpn.* **1982**, *55*, 2697.
(45) Dawson, W. R.; Kropp, J. L. *J. Opt. Soc. Am.* **1965**, *55*, 822.
(46) Bünzli, J.-C. G.; Yersin, J.-R. *Inorg. Chim. Acta* **1984**, *94*, 301.
(47) Haas, Y.; Stein, G. *J. Phys. Chem.* **1971**, *75*, 3668.
(48) Blasse, G. *Struct. Bonding* **1976**, *26*, 45.
(49) Bünzli, J.-C. G.; Ihringer, F. *Inorg. Chim. Acta* **1996**, *246*, 195.
(50) Bünzli, J.-C. G.; Froidevaux, P.; Harrowfield, J. M. *Inorg. Chem.* **1993**, *32*, 3306.
(51) Steemers, F. J.; Verboom, W.; Reinhoudt, D. N.; Vandertol, E. B.; Verhoeven, J.W. *J. Am. Chem. Soc.* **1995**, *117*, 9408.

Table 8. Lifetime (μs) of the $^5D_0$(Eu) Level in $[Eu(NO_3)_3(L^i)(solv)_x](solv')_y$ versus Temperature, Measured under Excitation through the Maximum of the $^5D_0 \leftarrow {}^7F_0$ Transition and through the Ligand Levels

	$^5D_0 \leftarrow {}^7F_0$ transition			ligand levels		
compd, L^i	10 K	77 K	295 K	10 K	77 K	295 K
2, L^1 [a]	829 ± 19	798 ± 11	709 ± 20	860 ± 50	840 ± 40	820 ± 40
3, L^3 [a]	1060 ± 40	1120 ± 30	1100 ± 40	*b*	1350 ± 40	1150 ± 40
4, L^4	1150 ± 30	1160 ± 30	900 ± 21	1180 ± 70	1200 ± 70	872 ± 35
5, L^6 [c]	923 ± 28	888 ± 37	952 ± 10 1110 ± 10	1240 ± 60	1190 ± 40	1250 ± 10
6, L^7	1330 ± 30	1320 ± 40	1110 ± 20	*b*	*b*	1160 ± 40
7, L^8	986 ± 30	897 ± 19	*d*	991 ± 30	*b*	*d*

[a] Partly from ref 9; data at 4 K instead of 10 K. [b] Not measured. [c] Two $^5D_0 \leftarrow {}^7F_0$ transitions at 295 K: 579.45 and 580.15 nm. [d] Signal too weak to be measured.

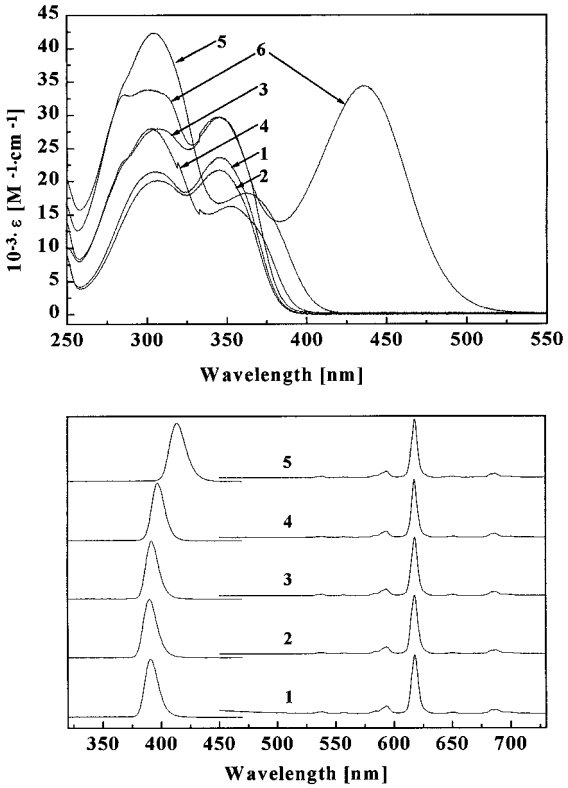

Figure 3. Absorption (top) and excitation and emission (bottom) spectra of 10^{-3} M $[Eu(NO_3)_3(L^i)]$ in degassed and anhydrous acetonitrile: 1, L^1; 2, L^3; 3, L^4; 4, L^6; 5, L^7; 6, L^8.

are 6−16 times smaller than the quantum yield of $Eu(NO_3)_3$ in the same solvent, determined upon excitation through the $^5D_0 \leftarrow {}^7F_0$ transition.[46] The bis(benzimidazolyl)pyridine bonded to Eu^{III} is apparently responsible for this reduction in quantum yield. Since the $^5D_0$(Eu) lifetime is almost temperature independent (*vide supra*), the influence of vibrations in the quenching mechanisms is small, henceforth pointing to the mixing between 4f and ligand states as being accountable for the additional radiationless processes. If this were true, direct excitation of the Eu^{III} ion should lead to similar quantum yield data. This has unfortunately not been possible to measure since the only Eu^{III} absorption with sufficient intensity ($^5L_6 \leftarrow {}^7F_{0,1}$) to carry out the experiment has a smaller absorbance at 395 nm (ϵ, *ca.* 5 $M^{-1}\cdot cm^{-1}$) than the bonded ligands.

In an effort to unravel the role played by the ligand in the decrease of the quantum yields, we have determined the quantum yields of the ligand-centered luminescence in the 1:1 and 1:3 La^{III} complexes with L^1 10^{-4} M in acetonitrile, relative to a 10^{-4} M solution of L^1. The excitation spectrum of L^1 presents two sharp bands corresponding to the 0-phonon transitions of the $^*\pi \leftarrow \pi$ transition listed in Table 5 and to a second $^*\pi \leftarrow \pi$ transition occurring in the UV, while the excitation spectra of the La^{III} complexes display three sharp bands corresponding the 0-phonon transitions of the three observed $^*\pi \leftarrow \pi$ transitions, the low-energy $^*\pi \leftarrow \pi$ transition of the ligand being split into two components upon complexation.[9,10] We discuss here the quantum yield obtained upon excitation onto the lower $^1\pi\pi^*$ state only. Indeed, at 10^{-4} M concentration, there is an appreciable dissociation of the complexes: the average number of coordinated ligands per La^{III} ion is 0.46 and 2.85 for the 1:1 and 1:3 complexes, respectively.[52] Excitation at 265 nm, through the more energetic $^*\pi \leftarrow \pi$ transition, results in exciting both the free and bonded ligand molecules. To determine the luminescence emitted by the complexes, the total luminescence measured has then to be corrected for the luminescence from the free ligand, which is much more important, and this process leads to large uncertainties, especially that part of the free ligand luminescence may be reabsorbed by the bonded ligand molecules. As a matter of fact, the binding of L^1 to La^{III} reduces the quantum yield of the lower energy $^1\pi\pi^*$ state by factors of 7 and 11 in the 1:1 and 1:3 complexes, respectively. Therefore, the decrease in quantum yield of the Eu-centered luminescence in going from the 1:1 to the 1:3 complex may be partly attributed to a decrease in the quantum yield of the ligand-centered luminescence. The measured luminescence comprises the emission from the $^3\pi\pi^*$ state, which is quite faint. The ratio $I(^3\pi\pi^*)/I(^1\pi\pi^*)$ could be roughly estimated by time-resolved luminescence at 77 K on frozen solutions to 2×10^{-4} for free L^1 and to 5×10^{-3} for bonded L^1.

Table 9. Quantum Yields of $^5D_0$(Eu) in $[Eu(NO_3)_3(L^i)(solv)_x]$ Solutions in Acetonitrile at 295 K Measured Relative to 10^{-3} M $[Eu(terpy)_3](ClO_4)_3$ (Q_{rel})

compd, L^i	concn ($mol\cdot L^{-1}$)	λ_{exc} (nm)	$\epsilon(\lambda_{exc})$ ($M^{-1}\cdot cm^{-1}$)	Q_{rel}	ref
$[Eu(terpy)_3]^{3+}$	10^{-3}	371	549	1.00[a]	*b*
2, L^1	10^{-3}	391	536	2.16	*b*
		377	5478	2.34	
$[Eu(L^1)_3]^{3+}$	10^{-3}	414	na	6.3×10^{-5}	11
3, L^3	10^{-3}	390	547	2.51	*b*
	10^{-4}	376	5352	2.74	
$[Eu(L^3)_3]^{3+}$	10^{-3}	419	na	4.8×10^{-4}	11
4, L^4	10^{-3}	392	556	2.86	*b*
	10^{-4}	379	5066	3.15	
$[Eu(L^4)_3]^{3+}$	10^{-3}	416	na	2.2×10^{-3}	11
5, L^6	10^{-3}	397	566	3.26	*b*
	10^{-4}	384	4945	3.82	
6, L^7	10^{-3}	413	623	1.31	*b*
	10^{-4}	396	5485	1.81	
$[EuZn(L^9)_3]^{5+}$	10^{-3}	442	530	1×10^{-4}	12
$[EuZn(L^{10})_3]^{5+}$	10^{-3}	395	555	0.13	12

[a] Absolute quantum yield: 1.3% (determined with respect to $[Ru(bipy)_3]^{2+}$. [b] This work.

(52) Petoud, S.; Bünzli, J.-C. G.; Piguet, C. Unpublished work, 1996.

The quantum yield variation of the Eu-centered luminescence for 1:1 nitrato complexes is in the order $L^6 > L^4 > L^3 > L^1 > L^7 \gg L^8$. The reason for the position of L^7 and L^8 in this series has been discussed above. Moreover, the relative position of L^1, L^3, and L^4 is the same as that for the triple helical edifices.[11] A detailed understanding of the substituent effect on the quantum yield is, however, difficult to gain in view of the variety of quenching processes intervening in the characterization of this parameter. For the $[Eu(L^i)_3]^{3+}$ helicates, the ligand stacking in the triple helical structure obviously plays a dominant role. This cannot evidently be the case for the 1:1 nitrato complexes. We note that the quantum yield increases when the methyl groups in L^1 are successively replaced by octyl and dimethoxybenzyl moieties and, comparing L^6 with L^4, that the introduction of a phenyl substituent in the 4-position of the central pyridine unit results in a further increase in the quantum yield. We assume this outcome mainly arises from the mixing of the ligand wave functions with 4f functions which affect both the energy transfer and the quenching processes rather than from inductive effects influencing the strength of the Eu−ligand bonds, since substituents with opposite electronic effects instigate similar changes in the quantum yield. In this respect, the position of the ligand $^3\pi\pi^*$ state (Table 9) certainly plays a nonnegligible role since the quantum yield increases when the energy gap between this state and the $^5D_0$ level decreases, with the exceptions of L^7 and L^8 for which the low-lying electronic levels appear to be a more determining factor contributing to the quenching of the metal-centered luminescence.

The quantum yields of 10^{-4} M solutions are systematically larger than those of 10^{-3} M solutions. Concentration quenching is a commonly observed phenomenon caused by reabsorption of the emitted light or by collisional deexcitation. Reabsorption can be ruled out in our case since the ligand absorbs at energy higher than the emitted light and since the only f−f transition able to reabsorb the Eu^{III} emission, $^5D_0 \leftarrow {}^7F_0$, has an extremely low oscillator strength ($\epsilon < 10^{-2}$ $M^{-1}\cdot cm^{-1}$). Decrease in collisional deactivation will account for the 8−17% increase in quantum yield detected for the complexes with ligands L^1, L^3, L^4, and L^6 but probably not for the 38% increase observed for the complex with L^7. In this case, partial decomplexation upon dilution could play a substantial role, as reported for the 1:3 triple helical edifices. Moreover, a recent study on the sensitization of Eu luminescence by benzoates has shown that $^3\pi\pi^*$ states of bonded ligands are less effective in transferring energy to the metal ion than $^3\pi\pi^*$ states of free ligands.[53]

Conclusion

The good fit observed between the tridentate coordination "cavity" of the bis(benzimidazolyl)pyridines and the trivalent lanthanide ions[9−11] is confirmed by the analysis of the crystal structure of $[Eu(NO_3)_3(L^7)(MeCN)]\cdot 2.5MeCN$ for which short Eu−N contacts are observed with the three N-atoms of the meridionally coordinated ligand (2.57 Å). The nature of the R^1 and R^2 substituents of ligands L^i influences both the arrangement of the inner coordination sphere of the metal ion and the crystal packing, mainly governed by strong intermolecular interactions involving π-stackings and O···H interactions with the nitrate ions, and by numerous weaker intermolecular interactions. The luminescence of the $^5D_0$(Eu) level in both the 1:1 nitrato complexes, the properties of which are reported in this paper, and the 1:3 triple-helical edifices $[Eu(L^i)]^{3+}$ [10,11] is influenced by several parameters. The more important include the ligand arrangement around the metal ion and for the 1:3 complexes the strong π-stacking interactions occurring between the ligand strands, the energy of the singlet and triplet states of the ligands and of the ligand-to-metal charge-transfer (LMCT) state, and vibronic couplings contributing to radiationless deactivation. Since f−f transitions are forbidden and since the ^7F_J(Eu) wave functions are relatively pure,[54] a minute admixture of other functions (vibronic, LMCT, ligand states) will dramatically alter the transition probability. Quantum yields will of course be dramatically affected by these admixtures. The data reported in this study demonstrate, however, that provided one considers a series of structurally similar complexes, a certain degree of rationalization can be met on the basis of simple considerations, such as the energy of the ligand levels and the substituent effect of the ligands. Despite the low quantum yields obtained for the 1:1 nitrato complexes, the benzimidazole-substituted pyridines appear to be versatile and well-adapted ligands for the design of lanthanide probes. A report on the determination of the substituent effect on the stability of the $[Ln(L^i)_m]^{3+}$ complexes will be published shortly.

Acknowledgment. We gratefully acknowledge Ms. Véronique Foiret, Ms. Christine Saint-Léger, and Mr. Huges Siegenthaler for their technical assistance. C.P. thanks the Werner Foundation for a fellowship, and J.-C.G.B. thanks the Fondation Herbette (Lausanne) for the gift of spectroscopic equipment. This work is supported through grants from the Swiss National Science Foundation.

Supporting Information Available: Tables describing detailed crystallographic data, atomic positional parameters, anisotropic displacement parameters, least-squares planes, and intermolecular interactions and figures showing crystal packing intermolecular interactions, the Eu($^5D_0 \rightarrow {}^7F_J$,$J$=0−4) emission spectra, and the Eu($^5D_0 \leftarrow {}^7F_0$) excitation spectra (15 pages). Ordering information is given on any current masthead page.

IC961305A

(53) Schrott, W.; Büchner, H.; Steiner, U. *J. Inf. Rec. Mater.* **1996**, *23*, 79.

(54) Porcher, P.; Caro, P. *J. Luminesc.* **1980**, *21*, 207.